Universität Karlsruhe (TH)
Institut für Baustatik

An enhanced FSDT model for the calculation of interlaminar shear stresses in composite plate structures

M. Schürg, W. Wagner, F. Gruttmann

Mitteilung 2(2009)

Universität Karlsruhe (TH)
Institut für Baustatik

An enhanced FSDT model for the calculation of interlaminar shear stresses in composite plate structures

M. Schürg, W. Wagner, F. Gruttmann

Mitteilung 2(2009)

Prof. Dr.–Ing. W. Wagner
Institut für Baustatik
Universität Karlsruhe
Postfach 6980
76128 Karlsruhe

Telefon: (0721) 608–2280
Telefax: (0721) 608–6015
E–mail: bs@.uni-karlsruhe.de
Internet: http://www.bs.uni-karlsruhe.de

An enhanced FSDT model for the calculation of interlaminar shear stresses in composite plate structures

M. Schürg*, W. Wagner+, F. Gruttmann*

* Fachgebiet Festkörpermechanik, Technische Universität Darmstadt, Hochschulstr. 1, 64289 Darmstadt, Germany

+ Institut für Baustatik, Universität Karlsruhe (TH), Kaiserstr. 12, 76131 Karlsruhe, Germany

Summary In this paper a procedure is proposed to calculate the interlaminar shear stresses in layered composite plates. The transverse shear stresses are obtained via the constitutive law and derivatives of some warping functions. For 4-node elements the derivatives of curvatures and strains of the reference surface with respect to the in-plane coordinates are determined through a system of four equations. Hence the equilibrium equations lead to a coupled system of ordinary differential equations, which are solved applying a displacement method. The resulting interlaminar shear stresses are continuous at the layer boundaries. The quality of the obtained results is demonstrated within several plate examples with symmetric and unsymmetric lay-ups. Comparisons with two other approaches using 9-node elements and a solid shell formulation together with a three-dimensional material law show good accuracy and efficiency of the proposed algorithm.

Key words: Layered composite structures, interlaminar shear stresses, warping function, displacement method

1 Introduction

Plate or shell theories are usually used to describe the overall deformation behaviour of thin laminated structures. Starting with formulations based on the classical laminate theory (CLT), nowadays the first-order shear deformation theory (FSDT) is the accepted basis to develop elements, see e.g. [1]. This theory is able to describe also the shear deformation behaviour, which is essential in the context of composite structures. It needs only C^0- instead of C^1-continuity, being of great interest from a numerical point of view. Often this approach gives satisfactory results for a wide class of structural problems, even for moderately thick laminates and should be the best compromise between prediction ability and computational costs, see e.g. Rohwer [2].

However if one is interested in more local problems -e.g. the question of construction of connections or the description of the interlaminar stresses- the use of above two-dimensional models is not appropriate. Highly complicated inter- and intralaminar failure modes (e.g. delamination and ply failure) may occur in laminated structures which could influence the overall structural behaviour strongly. An example of dealing with these problems is the international project COCOMAT, described e.g. in Degenhardt et.al. [3]. Furthermore, we mention a general survey on the computation of interlaminar stress concentrations, see Mittelstedt and Becker [4].

In the following we would like to concentrate on the question how to calculate interlaminar stresses. Within a finite element context this leads directly to the use of brick elements or

so-called solid shell elements for each layer, the introduction of layer-wise formulations, the use of higher order elements or the enhancement of plate or shell formulations. Advanced formulations exist, which allow the description of the bending behaviour of thin structures in an accurate way, see e.g. [5], [6], [7], among many others. Each layer is discretized with several elements ($\approx 5-10$) in thickness direction. The price for this type of modeling is a large number of unknowns leading to unacceptable computing times. Especially for non-linear problems with a multiplicity of load steps and several iterations in each load step this is not a feasible approach.

Another approach is given with a layer-wise theory. Here, the displacement field in each layer is represented separately, see e.g. Reddy [8]. In an early method of Chaudhuri [9] the formulation is limited to triangular elements and the calculation of the transverse shear stresses in thick composite plates. With the development of so-called zig-zag theories, piecewise polynomial distributions of the membrane displacements in thickness direction are evolved. This is achieved through the implementation of additional variables for each layer, so that the effort corresponds to the use of brick elements. Carrera [10] uses a mixed variational method to develop an element formulation that delivers transverse shear stresses for the laminate. A similar shell formulation is presented in Brank and Carrera [11]. For an overview of zig-zag theories for multilayered plates and shells see e.g. Carrera [12]. Developments of the authors on this topic have been published e.g. in [13], [14], [15] and [16]. Again these formulations lead to an effort in the range of a full 3D-computation, see e.g. Robbins and Reddy [17]. Thus, the practical application may be limited to detail investigations.

Another possibility to obtain transverse shear stresses is the application of higher order laminate theories. For example, Reddy [18] accounts for a parabolic distribution of the transverse shear strains through the thickness of the plate. Engblom and Ochoa [19] develop an element for a second-order composite laminate theory. These theories are usually named HSDT (Higher-order Shear Deformation Theory). Many finite elements (mostly linear plate formulations) have been proposed based on HSDT models. However, these methods need often C^1-continuous shape functions, which are less suitable for modern finite element models. Among many others we mention the papers of Reddy [20], Rao and Meyer-Piening [21] and Topdar et.al. [22].

Finally, post-processing or similar techniques can be used in conjunction with 2D finite elements. Thus results of commercial codes could be used as well as an implementation in a plate or shell element. The latter choice is preferable, if one is interested in an associated non-linear failure analysis of the structure. Besides the predictor corrector approach, e.g. [23], the equilibrium equations have been successfully exploited, e.g. [24]. In general, this requires higher-order shape functions to allow for second order derivatives of the in-plane stresses. Thus typically elements with bi-quadratic or bi-cubic shape functions are used, e.g. [25]. In order to ease this deficiency, having in mind the use of low order finite element formulations, further assumptions have to be introduced. Here a number of publications exist and we mention only a few of them. Rolfes and Rohwer [26] calculate the distribution of the transverse shear stresses in linear layered plates. They solve the equilibrium equations under the assumption of cylindrical bending. Furthermore the membrane forces are neglected in the constitutive equations. Auricchio and Sacco [1] present a 4-node finite-element based on a mixed-enhanced approach. Enhanced incompatible modes are used to improve the in-plane deformation and bubble functions for the rotational degrees of freedom. Additionally, functions link the transverse displacement to the rotations.

As stated above the use of brick elements or solid shell elements with a sufficient fine discretization in thickness direction leads to unreasonable large computing times. This is the motivation for the proposed plate and shell formulation which is characterized by the following features.

(i) An essential goal is to develop an interface to a 4–node plate or shell element, where the shear forces are obtained from the constitutive equations. Here, the formulation is implemented in a 5/6-parameter mixed-hybrid shell formulation [28].

(ii) The above mentioned assumptions of cylindrical bending and neglect of membrane forces in the constitutive equations are not used. For the 4-node element version (model 1) the derivatives of the membrane strains and curvatures are determined via a regularized minimum problem. Furthermore a special solution for symmetric laminates is proposed. Within the 9-node element version (model 2) the strain derivatives are computed from the displacement field.

(iii) A displacement method is developed to determine discrete values of two warping functions. The procedure is computationally very effective, since the sparse stiffness matrix has to be set up and factorized only once for a laminate with fixed lay-up. The transverse shear stresses are obtained via the constitutive law and derivatives of the warping function.

(iv) The transverse shear stresses are continuous at the layer boundaries. For the 4–node element version applied to symmetric laminates the integration of the transverse shear stresses through the thickness yields the shear forces exactly. The exact fulfilment of stress boundary conditions at the lower and upper surface holds also for this model. Within the other element versions the conditions are approximately fulfilled.

The paper is organized as follows. In section 2 we present the basic equations of laminated plates. In section 3 the derivatives of membrane strains and curvatures are determined for 4–node elements and 9–node elements. A coupled system of ordinary differential equations in terms of two warping functions is formulated and solved for an individual layer in section 4. The solution for the total laminate is obtained applying a displacement method. The computed results are discussed in section 5 for several plate examples with symmetric and unsymmetric lay-ups.

2 Basic equations

We consider a laminated plate with n layers. A cartesian coordinate system is introduced in the reference surface of the plate, see Fig. 1. Within each layer a normalized coordinate ζ in thickness direction is defined with $0 \leq \zeta \leq 1$, see Fig. 2. The total thickness of the plate is denoted by H, whereas top and bottom surface are described with the z-coordinate h^+ and h^-. Note, that the reference surface can be chosen arbitrarily. In most cases the mid-surface of the plate is used as reference surface leading to $h^+ = H/2$ and $h^- = -H/2$.
The membrane strains ε_x and ε_y, the shear strain ε_{xy} and curvatures of the plate κ_x, κ_y and κ_{xy} are defined within a Reissner-Mindlin kinematic

$$\boldsymbol{\varepsilon} = \begin{bmatrix} \varepsilon_x \\ \varepsilon_y \\ \varepsilon_{xy} \end{bmatrix} = \begin{bmatrix} u_{x,x} \\ u_{y,y} \\ u_{x,y} + u_{y,x} \end{bmatrix} \qquad \boldsymbol{\kappa} = \begin{bmatrix} \kappa_x \\ \kappa_y \\ \kappa_{xy} \end{bmatrix} = \begin{bmatrix} \beta_{x,x} \\ \beta_{y,y} \\ \beta_{x,y} + \beta_{y,x} \end{bmatrix}, \tag{1}$$

where u_x, u_y are the in-plane displacements of the reference surface and β_x, β_y describe the slopes of deformed cross sections. Commas denote partial derivatives with respect to x and y. Hence the layer strains follow from the kinematic assumption

$$\bar{\boldsymbol{\varepsilon}} = \boldsymbol{\varepsilon} + z\,\boldsymbol{\kappa}\,. \tag{2}$$

Furthermore, the transverse shear strains $\bar{\gamma}_{xz}$ and $\bar{\gamma}_{yz}$ are introduced as derivatives of some warping functions $\varphi_x(z)$ and $\varphi_y(z)$

$$\begin{array}{rcl} \bar{\gamma}_{xz} & := & \varphi_{x,z}(z) \\ \bar{\gamma}_{yz} & := & \varphi_{y,z}(z) \end{array} \tag{3}$$

which are assumed to be functions of the thickness coordinate. A typical shape of the warping function $\varphi_x(z)$ is depicted for a cross-ply laminate with 5 layers in Fig. 2.

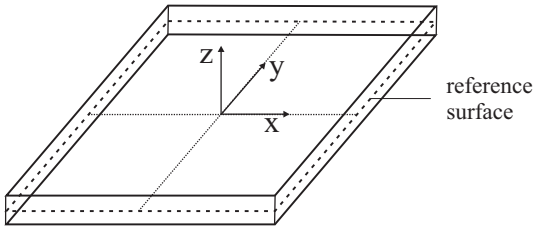

Figure 1: Plate with coordinate system

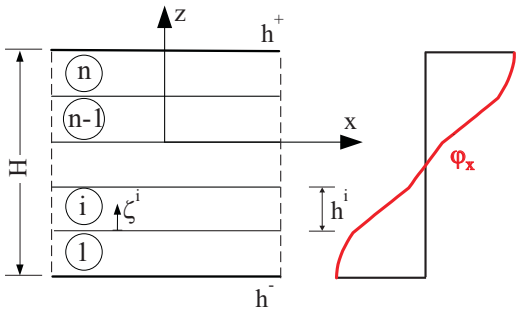

Figure 2: Layered composite plate

Neglecting body forces the equilibrium equations are written for the x- and y-direction

$$\begin{array}{l} \sigma_{x,x} + \tau_{xy,y} + \tau_{xz,z} = 0 \\ \sigma_{y,y} + \tau_{xy,x} + \tau_{yz,z} = 0\,. \end{array} \tag{4}$$

In (4) the normal stresses σ_x, σ_y, and the shear stresses τ_{xy} as well as transverse shear stresses τ_{xz} and τ_{yz} enter.
Constitutive equations assuming transversal isotopic material behaviour are introduced in the following standard manner

$$\begin{bmatrix} \sigma_x \\ \sigma_y \\ \tau_{xy} \end{bmatrix} = \begin{bmatrix} C_{11} & C_{12} & C_{13} \\ C_{21} & C_{22} & C_{23} \\ C_{31} & C_{32} & C_{33} \end{bmatrix} \begin{bmatrix} \bar{\varepsilon}_x \\ \bar{\varepsilon}_y \\ \bar{\varepsilon}_{xy} \end{bmatrix} \qquad \begin{bmatrix} \tau_{xz} \\ \tau_{yz} \end{bmatrix} = \begin{bmatrix} C_{44} & C_{45} \\ C_{54} & C_{55} \end{bmatrix} \begin{bmatrix} \bar{\gamma}_{xz} \\ \bar{\gamma}_{yz} \end{bmatrix} \tag{5}$$

$$\boldsymbol{\sigma} = \mathbf{C}\,\bar{\boldsymbol{\varepsilon}} \qquad\qquad \boldsymbol{\tau} = \mathbf{C}_s\,\bar{\boldsymbol{\gamma}}\,.$$

Due to the varying fiber orientation the material constants $C_{ij} = C_{ji}$ differ for each individual layer. To alleviate the notation the layer index i is omitted. Inserting the constitutive equations (5) into the equilibrium equations (4) yields

$$\begin{aligned} \begin{bmatrix} \tau_{xz,z} \\ \tau_{yz,z} \end{bmatrix} + \begin{bmatrix} b_x \\ b_y \end{bmatrix} &= \begin{bmatrix} 0 \\ 0 \end{bmatrix} & \qquad \begin{bmatrix} b_x \\ b_y \end{bmatrix} &= \begin{bmatrix} \sigma_{x,x} + \tau_{xy,y} \\ \sigma_{y,y} + \tau_{xy,x} \end{bmatrix} \\ \boldsymbol{\tau}_{,z} + \mathbf{b} &= \mathbf{0} & \qquad \mathbf{b} &= \mathbf{B}\,\mathbf{x} \end{aligned} \tag{6}$$

with

$$\mathbf{B} = \begin{bmatrix} \mathbf{C}_1 & \mathbf{C}_3 & z\,\mathbf{C}_1 & z\,\mathbf{C}_3 \\ \mathbf{C}_3 & \mathbf{C}_2 & z\,\mathbf{C}_3 & z\,\mathbf{C}_2 \end{bmatrix} \qquad \mathbf{x} = \begin{bmatrix} \boldsymbol{\varepsilon}_{,x} \\ \boldsymbol{\varepsilon}_{,y} \\ \boldsymbol{\kappa}_{,x} \\ \boldsymbol{\kappa}_{,y} \end{bmatrix} \tag{7}$$

$$\mathbf{C}_1 = [C_{11}, C_{12}, C_{13}]\,, \qquad \mathbf{C}_2 = [C_{21}, C_{22}, C_{23}]\,, \qquad \mathbf{C}_3 = [C_{31}, C_{32}, C_{33}]\,.$$

The derivatives of the membrane strains and curvatures with respect to x and y are determined in the following section.

3 Derivatives of membrane strains and curvatures

Different procedures for 4-node elements (model 1) with bi-linear shape functions and for 9-node elements (model 2) with bi-quadratic shape functions are developed in this section.

3.1 Model 1: 4-node element

3.1.1 Regularized minimum problem

The vector $\mathbf{x}$ of strain derivatives is determined via a regularized minimum problem since second derivatives of the displacement fields can not be computed from bi-linear shape functions. For this purpose we setup a system of four equations. The first two equations describe the stress boundary conditions at the upper surface of the laminate. They are obtained by integration of (4) with respect to z and incorporation of (6):

$$\begin{aligned} \begin{bmatrix} \tau_{xz}(z = h^+) \\ \tau_{yz}(z = h^+) \end{bmatrix} &= \begin{bmatrix} \tau_{xz}(z = h^-) \\ \tau_{yz}(z = h^-) \end{bmatrix} - \int_{h^-}^{h^+} \begin{bmatrix} b_x \\ b_y \end{bmatrix} dz = \begin{bmatrix} 0 \\ 0 \end{bmatrix} \\ \boldsymbol{\tau}(z = h^+) &= \boldsymbol{\tau}(z = h^-) - \int_{h^-}^{h^+} \mathbf{B}\,dz\,\mathbf{x} = \mathbf{0}\,. \end{aligned} \tag{8}$$

At the lower surface the stress boundary condition $\boldsymbol{\tau}(z = h^-) = \mathbf{0}$ is fulfilled by the below presented displacement method. The third and fourth equation describe the definition of the shear forces q_x and q_y

$$\int_{h^-}^{h^+} \begin{bmatrix} \tau_{xz} \\ \tau_{yz} \end{bmatrix} dz = \begin{bmatrix} q_x \\ q_y \end{bmatrix}. \tag{9}$$

Considering eqs. (4) and (6) leads to

$$\int_{h^-}^{h^+} \begin{bmatrix} \tau_{xz} \\ \tau_{yz} \end{bmatrix} dz = \int_{h^-}^{h^+} \begin{bmatrix} \tau_{xz} + z(\sigma_{x,x} + \tau_{xy,y} + \tau_{xz,z}) \\ \tau_{yz} + z(\sigma_{y,y} + \tau_{xy,x} + \tau_{yz,z}) \end{bmatrix} dz = \underbrace{\begin{bmatrix} z\,\tau_{xz} \\ z\,\tau_{yz} \end{bmatrix}_{h^-}^{h^+}}_{\mathbf{0}} + \int_{h^-}^{h^+} \begin{bmatrix} b_x \\ b_y \end{bmatrix} z\,dz \tag{10}$$

thus

$$\int_{h^-}^{h^+} \boldsymbol{\tau}\, dz = \int_{h^-}^{h^+} \mathbf{B}\, z\, dz\, \mathbf{x} = \mathbf{q}\,. \tag{11}$$

Introducing

$$\mathbf{A} := \int_{h^-}^{h^+} \begin{bmatrix} \mathbf{B} \\ z\,\mathbf{B} \end{bmatrix} dz\,, \qquad \tilde{\mathbf{q}} = \begin{bmatrix} \mathbf{0} \\ \mathbf{q} \end{bmatrix} \tag{12}$$

eqs. (9) and (12) can be summarized as

$$\mathbf{A}\,\mathbf{x} = \tilde{\mathbf{q}}\,. \tag{13}$$

This under-determined system of equations is approximately solved via a regularized minimum problem

$$\frac{1}{2}\,\mathbf{r}^T\mathbf{r} + \frac{\alpha}{2}\,\mathbf{x}^T\mathbf{x} \quad \rightarrow \quad \min \tag{14}$$

where $\mathbf{r} = \mathbf{A}\,\mathbf{x} - \tilde{\mathbf{q}}$ denotes the residual vector and $\alpha > 0$ is a regularization parameter. Minimization yields

$$(\mathbf{A}^T\mathbf{A} + \alpha\,\mathbf{1})\,\mathbf{x} = \mathbf{A}^T\tilde{\mathbf{q}} \tag{15}$$

where $\mathbf{1}$ is a twelfth order unit matrix. The regularization is necessary, since $\mathbf{A}^T\mathbf{A}$ is with 4 non-zero eigenvalues rank deficient. The parameter $\alpha = Z\,\alpha^*$ is normalized by a factor $Z = [H^2 \sum_{i=1}^{n} 0.5\,(C_{44} + C_{55})h^i]^2$, which is motivated by eqs. (5), (7), (12) and (15). An investigation concerning the sensitivity of the normalized parameter α^* on the solution is given in section 5.5. With a sufficient large α using floating point arithmetic the system of equations (15) is regular and can be solved for $\mathbf{x}$.

3.1.2 Special solution for symmetric laminates

Symmetric laminates are characterized by decoupling of membrane and bending behaviour. Hence for transverse loading the in–plane strains vanish identically, thus $\boldsymbol{\varepsilon} \equiv \mathbf{0}$. Accordingly, the derivatives of $\boldsymbol{\varepsilon}$ with respect to x and y also vanish

$$\boldsymbol{\varepsilon}_{,x} = \mathbf{0}\,, \qquad\qquad \boldsymbol{\varepsilon}_{,y} = \mathbf{0}\,. \tag{16}$$

A rotation of the coordinate system with angle φ is introduced as follows

$$\begin{bmatrix} \hat{x} \\ \hat{y} \end{bmatrix} = \begin{bmatrix} c & s \\ -s & c \end{bmatrix} \begin{bmatrix} x \\ y \end{bmatrix} \qquad\qquad \begin{aligned} s &:= \sin\varphi \\ c &:= \cos\varphi\,. \end{aligned}$$
$$\hat{\mathbf{x}} = \mathbf{T}\,\mathbf{x}\,. \tag{17}$$

This leads to the transformation of the curvatures, see e.g. [27] for membrane strains

$$\begin{bmatrix} \hat{\kappa}_x \\ \hat{\kappa}_y \\ \hat{\kappa}_{xy} \end{bmatrix} = \begin{bmatrix} c^2 & s^2 & sc \\ s^2 & c^2 & -sc \\ -2sc & 2sc & c^2 - s^2 \end{bmatrix} \begin{bmatrix} \kappa_x \\ \kappa_y \\ \kappa_{xy} \end{bmatrix} \tag{18}$$

$$\hat{\boldsymbol{\kappa}} = \hat{\mathbf{T}}\,\boldsymbol{\kappa}$$

and in a straight forward way to the transformations of the stiffness matrices and shear forces

$$\hat{\mathbf{D}} = \hat{\mathbf{T}}^{-T}\,\mathbf{D}\,\hat{\mathbf{T}}^{-1} \qquad \hat{\mathbf{C}} = \hat{\mathbf{T}}^{-T}\,\mathbf{C}\,\hat{\mathbf{T}}^{-1} = \begin{bmatrix} \hat{\mathbf{C}}_1 \\ \hat{\mathbf{C}}_2 \\ \hat{\mathbf{C}}_3 \end{bmatrix} \qquad \hat{\mathbf{q}} = \mathbf{T}\,\mathbf{q} \tag{19}$$

with $\mathbf{D} = \int_{h^-}^{h^+} z^2\,\mathbf{C}\,dz$ and $\hat{\mathbf{q}} = [\hat{q}_x, \hat{q}_y]^T$. The angle φ is determined introducing the condition

$$\hat{\kappa}_{xy} = \hat{\beta}_{x,\hat{y}} + \hat{\beta}_{y,\hat{x}} = -2\,s\,c\,(\kappa_x - \kappa_y) + (c^2 - s^2)\,\kappa_{xy} \equiv 0 \tag{20}$$

which yields

$$\varphi = \frac{1}{2}\arctan\left(\frac{\kappa_{xy}}{\kappa_x - \kappa_y}\right). \tag{21}$$

The denominator in eq. (21) may take the value zero, however in the numerical computations this can be avoided by a small pertubation.
Since $\hat{\beta}_x$ and $\hat{\beta}_y$ are independent functions of $\hat{x}$ and $\hat{y}$ in general $\hat{\beta}_{x,\hat{y}} \neq -\hat{\beta}_{y,\hat{x}}$ holds, thus each term in (20) must vanish at any point of the plate

$$\begin{aligned} \hat{\beta}_{x,\hat{y}} &\equiv 0 \\ \hat{\beta}_{y,\hat{x}} &\equiv 0\,. \end{aligned} \tag{22}$$

In this case also the derivatives of $\hat{\kappa}_{xy}$ in (20) and $\hat{\beta}_{x,\hat{y}}$ and $\hat{\beta}_{y,\hat{x}}$ in (22) with respect to the coordinates $\hat{x}$ and $\hat{y}$ vanish

$$\begin{aligned} \hat{\kappa}_{xy,\hat{x}} &= 0 \\ \hat{\kappa}_{xy,\hat{y}} &= 0 \\ \hat{\kappa}_{x,\hat{y}} &= \hat{\beta}_{x,\hat{y}\hat{x}} = 0 \\ \hat{\kappa}_{y,\hat{x}} &= \hat{\beta}_{y,\hat{x}\hat{y}} = 0\,. \end{aligned} \tag{23}$$

Considering (16) and (23) equation (13) can now be reduced to a coupled system of two equations

$$\begin{bmatrix} \hat{D}_{11} & \hat{D}_{23} \\ \hat{D}_{13} & \hat{D}_{22} \end{bmatrix} \begin{bmatrix} \hat{\kappa}_{x,\hat{x}} \\ \hat{\kappa}_{y,\hat{y}} \end{bmatrix} = \begin{bmatrix} \hat{q}_x \\ \hat{q}_y \end{bmatrix} \tag{24}$$

and solved for the derivatives of the curvatures, and thus

$$\hat{\mathbf{x}} = [0, 0, 0, 0, 0, 0, \hat{\kappa}_{x,\hat{x}}, 0, 0, 0, \hat{\kappa}_{y,\hat{y}}, 0]^T. \tag{25}$$

With (25) we are able to compute

$$\mathbf{b} = \mathbf{T}^T\,\hat{\mathbf{b}} \qquad \hat{\mathbf{b}} = \hat{\mathbf{B}}\,\hat{\mathbf{x}} \qquad \hat{\mathbf{B}} = \begin{bmatrix} \hat{\mathbf{C}}_1 & \hat{\mathbf{C}}_3 & z\,\hat{\mathbf{C}}_1 & z\,\hat{\mathbf{C}}_3 \\ \hat{\mathbf{C}}_3 & \hat{\mathbf{C}}_2 & z\,\hat{\mathbf{C}}_3 & z\,\hat{\mathbf{C}}_2 \end{bmatrix} \tag{26}$$

Once $\mathbf{b}$ is obtained one can proceed in the section on the calculation of the transverse shear stresses. It is important to note that for the exception case $\hat{\beta}_{x,\hat{y}} = -\hat{\beta}_{y,\hat{x}}$ at singular points the model can not be applied.

3.2 Model 2: 9-node element

In this case all strain derivatives can be evaluated with second derivatives of the displacement field. Applying the isoparametric concept the first derivatives of the bi-quadratic shape functions $N_I(\xi,\eta)$ for 9-node elements $I = 1...9$ yields

$$\begin{bmatrix} x_{,\xi} & y_{,\xi} \\ x_{,\eta} & y_{,\eta} \end{bmatrix} \begin{bmatrix} N_{I,x} \\ N_{I,y} \end{bmatrix} = \begin{bmatrix} N_{I,\xi} \\ N_{I,\eta} \end{bmatrix} \tag{27}$$

with the Jacobi matrix

$$\begin{bmatrix} x_{,\xi} & y_{,\xi} \\ x_{,\eta} & y_{,\eta} \end{bmatrix} = \begin{bmatrix} J_{11} & J_{12} \\ J_{21} & J_{22} \end{bmatrix} = \sum_{I=1}^{9} \begin{bmatrix} N_{I,\xi}\, x_I & N_{I,\xi}\, y_I \\ N_{I,\eta}\, x_I & N_{I,\eta}\, y_I \end{bmatrix}. \tag{28}$$

Hence the second derivatives are given with the solution of the following system of equation and can be derived from (27) using (28) in a straight forward way applying product rule and chain rule of differentiation

$$\begin{bmatrix} J_{11}J_{11} & J_{12}J_{12} & 2J_{11}J_{12} \\ J_{21}J_{21} & J_{22}J_{22} & 2J_{21}J_{22} \\ J_{11}J_{21} & J_{12}J_{22} & J_{11}J_{22} + J_{12}J_{21} \end{bmatrix} \begin{bmatrix} N_{I,xx} \\ N_{I,yy} \\ N_{I,xy} \end{bmatrix} = \begin{bmatrix} N_{I,\xi\xi} - J_{11,\xi}\, N_{I,x} - J_{12,\xi}\, N_{I,y} \\ N_{I,\eta\eta} - J_{21,\eta}\, N_{I,x} - J_{22,\eta}\, N_{I,y} \\ N_{I,\xi\eta} - J_{11,\eta}\, N_{I,x} - J_{22,\xi}\, N_{I,y} \end{bmatrix}. \tag{29}$$

The derivatives of $J_{\alpha\beta}$ with respect to ξ and η can be directly computed from (28).

4 Calculation of the transverse shear stresses

With the membrane strain derivatives and curvature derivatives at hand one can proceed with the calculation of the warping functions φ_x, φ_y. This leads with Eqs. (3) – (6) to a coupled system of linear inhomogeneous ordinary differential equations

$$\begin{bmatrix} C_{44} & C_{45} \\ C_{54} & C_{55} \end{bmatrix} \begin{bmatrix} \varphi_{x,zz} \\ \varphi_{y,zz} \end{bmatrix} = - \begin{bmatrix} b_x \\ b_y \end{bmatrix} \tag{30}$$

In the following we specify the terms for a specific layer i, see Fig. 2. To alleviate the notation the index i is omitted in all terms. With $0 \le \zeta \le 1$ we parameterize the thickness coordinate $z = z_1 + \zeta h$, where z_1 denotes the coordinate of the bottom of the layer and h the thickness of the layer, respectively. Hence the right hand side in (30) is reformulated in terms of ζ

$$\begin{aligned} \begin{bmatrix} b_x \\ b_y \end{bmatrix} &= \begin{bmatrix} b_x^0 \\ b_y^0 \end{bmatrix} + \zeta \begin{bmatrix} b_x^1 \\ b_y^1 \end{bmatrix} \\ \mathbf{b} &= (\mathbf{B}_0 + \zeta\, \mathbf{B}_1)\, \mathbf{x} \end{aligned} \tag{31}$$

with

$$\mathbf{B}_0 = \begin{bmatrix} \mathbf{C}_1 & \mathbf{C}_3 & z_1\, \mathbf{C}_1 & z_1\, \mathbf{C}_3 \\ \mathbf{C}_3 & \mathbf{C}_2 & z_1\, \mathbf{C}_3 & z_1\, \mathbf{C}_2 \end{bmatrix} \qquad \mathbf{B}_1 = \begin{bmatrix} \mathbf{0} & \mathbf{0} & h\, \mathbf{C}_1 & h\, \mathbf{C}_3 \\ \mathbf{0} & \mathbf{0} & h\, \mathbf{C}_3 & h\, \mathbf{C}_2 \end{bmatrix}. \tag{32}$$

The solution of the system of differential equations (30) consists of a homogeneous and a particular solution with

$$\begin{array}{lll} \varphi_x = \varphi_x^h + \varphi_x^p & \varphi_x^h = c_{x1} + c_{x2}\zeta & \varphi_x^p = c_{x3}\zeta^2 + c_{x4}\zeta^3 \\ \varphi_y = \varphi_y^h + \varphi_y^p & \varphi_y^h = c_{y1} + c_{y2}\zeta & \varphi_y^p = c_{y3}\zeta^2 + c_{y4}\zeta^3 \,. \end{array} \tag{33}$$

The coefficients c_{x3}, c_{x4}, c_{y3} and c_{y4} are determined by inserting the particular solution into the system (30)

$$\begin{aligned} \begin{bmatrix} C_{44} & C_{45} \\ C_{54} & C_{55} \end{bmatrix} \begin{bmatrix} c_{x3} \\ c_{y3} \end{bmatrix} &= -\begin{bmatrix} b_x^0 \\ b_y^0 \end{bmatrix} \frac{h^2}{2} \\ \begin{bmatrix} C_{44} & C_{45} \\ C_{54} & C_{55} \end{bmatrix} \begin{bmatrix} c_{x4} \\ c_{y4} \end{bmatrix} &= -\begin{bmatrix} b_x^1 \\ b_y^1 \end{bmatrix} \frac{h^3}{6} \end{aligned} \tag{34}$$

which yields with $D = C_{44}C_{55} - C_{45}C_{54}$ the constants

$$\begin{aligned} c_{x3} &= -(b_x^0 C_{55} - b_y^0 C_{45})\frac{h^2}{2D} \\ c_{y3} &= -(b_y^0 C_{44} - b_x^0 C_{54})\frac{h^2}{2D} \\ c_{x4} &= -(b_x^1 C_{55} - b_y^1 C_{45})\frac{h^3}{6D} \\ c_{y4} &= -(b_y^1 C_{44} - b_x^1 C_{54})\frac{h^3}{6D} \,. \end{aligned} \tag{35}$$

The coefficients c_{x1}, c_{x2}, c_{y1} and c_{y2} of the homogeneous solution are expressed with the discrete values of φ_x and φ_y at the layer boundary

$$\begin{array}{lll} \varphi_{x1} = \varphi_x(0) & & c_{x1} = \varphi_{x1} \\ \varphi_{x2} = \varphi_x(1) & \rightarrow & c_{x2} = \varphi_{x2} - \varphi_{x1} - c_{x3} - c_{x4} \\ \varphi_{y1} = \varphi_y(0) & & c_{y1} = \varphi_{y1} \\ \varphi_{y2} = \varphi_y(1) & & c_{y2} = \varphi_{y2} - \varphi_{y1} - c_{y3} - c_{y4} \end{array} \tag{36}$$

Hence the quadratic shape of the shear stresses follows with (3) and (5) as derivative of the warping functions

$$\begin{aligned} \tau_{xz} &= C_{44}\,\varphi_{x,z} + C_{45}\,\varphi_{y,z} \\ &= \frac{C_{44}}{h}(c_{x2} + 2c_{x3}\zeta + 3c_{x4}\zeta^2) + \frac{C_{45}}{h}(c_{y2} + 2c_{y3}\zeta + 3c_{y4}\zeta^2) \\ \tau_{yz} &= C_{45}\,\varphi_{x,z} + C_{55}\,\varphi_{y,z} \\ &= \frac{C_{45}}{h}(c_{x2} + 2c_{x3}\zeta + 3c_{x4}\zeta^2) + \frac{C_{55}}{h}(c_{y2} + 2c_{y3}\zeta + 3c_{y4}\zeta^2) \end{aligned} \tag{37}$$

Evaluation of (37) at the layer boundaries considering the definitions according to Fig. 3 yields

$$
\begin{aligned}
\tau_{x1} = -\tau_{xz}(0) &= -\frac{C_{44}}{h}c_{x2} - \frac{C_{45}}{h}c_{y2} \\
&= \frac{C_{44}}{h}(\varphi_{x1} - \varphi_{x2} + c_{x3} + c_{x4}) + \frac{C_{45}}{h}(\varphi_{y1} - \varphi_{y2} + c_{y3} + c_{y4}) \\
\tau_{x2} = \tau_{xz}(1) &= \frac{C_{44}}{h}(c_{x2} + 2c_{x3} + 3c_{x4}) + \frac{C_{45}}{h}(c_{y2} + 2c_{y3} + 3c_{y4}) \\
&= \frac{C_{44}}{h}(\varphi_{x2} - \varphi_{x1} + c_{x3} + 2c_{x4}) + \frac{C_{45}}{h}(\varphi_{y2} - \varphi_{y1} + c_{y3} + 2c_{y4}) \\
\tau_{y1} = -\tau_{yz}(0) &= -\frac{C_{54}}{h}c_{x2} - \frac{C_{55}}{h}c_{y2} \\
&= \frac{C_{54}}{h}(\varphi_{x1} - \varphi_{x2} + c_{x3} + c_{x4}) + \frac{C_{55}}{h}(\varphi_{y1} - \varphi_{y2} + c_{y3} + c_{y4}) \\
\tau_{y2} = \tau_{yz}(1) &= \frac{C_{54}}{h}(c_{x2} + 2c_{x3} + 3c_{x4}) + \frac{C_{55}}{h}(c_{y2} + 2c_{y3} + 3c_{y4}) \\
&= \frac{C_{54}}{h}(\varphi_{x2} - \varphi_{x1} + c_{x3} + 2c_{x4}) + \frac{C_{55}}{h}(\varphi_{y2} - \varphi_{y1} + c_{y3} + c_{y4})
\end{aligned}
\tag{38}
$$

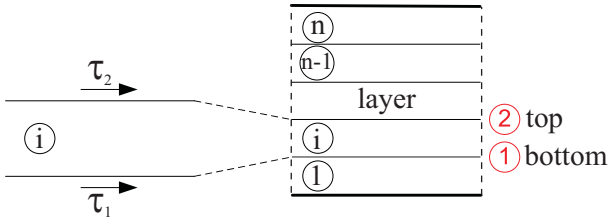

Figure 3: Definition of shear stresses at layer boundaries

Thus a system of equations can be established for each layer, where $\boldsymbol{\tau}_i$ contains the transverse shear stresses at top and bottom of the layer, $\boldsymbol{k}_i$ is an element stiffness matrix, $\mathbf{v}_i$ contains the unknown values of the warping functions at top and bottom of each layer and the vector $\mathbf{f}_i$ is written in terms of the constants defined in Eq. (31).

$$
\begin{aligned}
\begin{bmatrix} \tau_{x1} \\ \tau_{y1} \\ \tau_{x2} \\ \tau_{y2} \end{bmatrix} &= \frac{1}{h}\begin{bmatrix} C_{44} & C_{45} & -C_{44} & -C_{45} \\ C_{54} & C_{55} & -C_{54} & -C_{55} \\ -C_{44} & -C_{45} & C_{44} & C_{45} \\ -C_{54} & -C_{55} & C_{54} & C_{55} \end{bmatrix} \begin{bmatrix} \varphi_{x1} \\ \varphi_{y1} \\ \varphi_{x2} \\ \varphi_{y2} \end{bmatrix} - \frac{6}{h}\begin{bmatrix} 3\,b_x^0 + b_x^1 \\ 3\,b_y^0 + b_y^1 \\ 3\,b_x^0 + 2b_x^1 \\ 3\,b_y^0 + 2b_y^1 \end{bmatrix} \\
\boldsymbol{\tau}_i &= \mathbf{k}_i\,\mathbf{v}_i - \mathbf{f}_i\,.
\end{aligned}
\tag{39}
$$

Alternatively the vector $\mathbf{f}_i$ can also be written as

$$
\mathbf{f}_i = -\frac{1}{h}\begin{bmatrix} -C_{44}(c_{x3} + c_{x4}) & -C_{45}(c_{y3} + c_{y4}) \\ -C_{54}(c_{x3} + c_{x4}) & -C_{55}(c_{y3} + c_{y4}) \\ -C_{44}(c_{x3} + 2\,c_{x4}) & -C_{45}(c_{y3} + 2c_{y4}) \\ -C_{54}(c_{x3} + 2\,c_{x4}) & -C_{55}(c_{y3} + 2c_{y4}) \end{bmatrix}. \tag{40}
$$

The continuity of the shear stresses at all layer boundaries can be written as $\sum_{i=1}^{n} \mathbf{T}_i = \mathbf{0}$,

where $\mathbf{T}_i$ contains the transverse shear stresses at all layer boundaries, thus

$$\sum_{i=1}^{n} \mathbf{T}_i = \sum_{i=1}^{n} \mathbf{a}_i^T \boldsymbol{\tau}_i = \sum_{i=1}^{n} \mathbf{a}_i^T \mathbf{k}_i \mathbf{a}_i \mathbf{V} - \sum_{i=1}^{n} \mathbf{a}_i^T \mathbf{f}_i = \mathbf{0} \tag{41}$$

which yields the linear system of equations

$$\mathbf{K}\mathbf{V} = \mathbf{F} \tag{42}$$

Here, $\mathbf{K} = \sum_{i=1}^{n} \mathbf{a}_i^T \mathbf{k}_i \mathbf{a}_i$ is the assembled stiffness matrix and $\mathbf{F} = \sum_{i=1}^{n} \mathbf{a}_i^T \mathbf{f}_i$ the assembled load vector, respectively. The matrix $\mathbf{a}_i$ denotes the assembly matrix, thus $\mathbf{v}_i = \mathbf{a}_i \mathbf{V}$ holds. The sparse stiffness matrix $\mathbf{K}$ has to be set up and factorized only once for a laminate with fixed lay-up. Thus, the solution of (42) can be effectively computed applying only a back substitution, which then yields $\mathbf{V}$ with the discrete warping ordinates at the nodes. To prevent rigid body motions boundary conditions have to be imposed. We choose $\varphi_x(z = h^+) = 0$ and $\varphi_y(z = h^+) = 0$. A different choice of boundary conditions leads to a solution for φ_x and φ_y which differs by constants, however these constants do not affect the shear stresses.

Remark:
Within an alternative procedure eq. (6) could be integrated for each layer with respect to the thickness coordinate z, considering that $\mathbf{B}$ is a linear function of ζ. This requires as boundary condition knowledge of the shear stresses of the adjacent lower layer.
On the other hand once $\mathbf{V}$ is known, exploitation of eq. (39) allows calculation of the shear stresses of an individual layer without knowledge of the values of the adjacent layer.

5 Examples

The developed model 1 is implemented in a 5/6-parameter 4–node mixed shell element, see [28], within an extended version of the general finite element program FEAP [29] with embedded fast direct solver PARDISO for sparse systems [30]. The element formulation allows the calculation of the transverse shear stresses, once the stress resultants have been computed. We perform the stress evaluation at the element center. The material constants for transversal isotropy are chosen for all examples as:

$$\begin{aligned} E_1 &= 125000\, N/mm^2 & \qquad G_{12} &= 4800\, N/mm^2 \\ E_2 &= 7400\, N/mm^2 & \qquad G_{23} &= 2700\, N/mm^2 \\ \nu_{12} &= 0.34\,, \end{aligned}$$

where the index 1 refers to the preferred direction of the material. In example 1, 2 and 4 model 1 for symmetric laminates according to section 3.1.2 is applied. In example 3 the normalized regularization parameter α^* has been chosen as $\alpha^* = 10^{-10}$, see also section 5.5. For comparison we present also results obtained with a 9-node shell element (model 2) and results using a solid shell element with 8 nodes [6].

5.1 Example 1

With the first example the transverse shear stresses of a square plate ($l_x = l_y = 50\, mm$) with thickness $h = 1\, mm$ which is simply supported and subjected to a constant load of $1\, N/mm^2$ are evaluated.

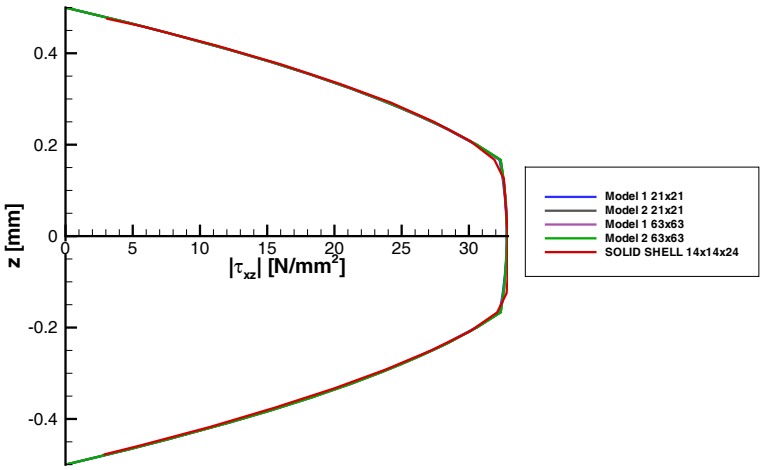

Figure 4: Shear stress $\tau_{xz}(x = 23.214, y = 1.786, z)$ for cross-ply lay-up 0/90/0

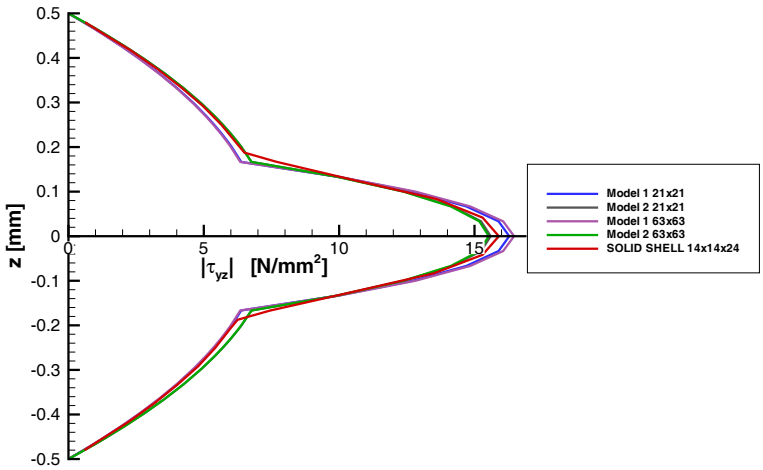

Figure 5: Shear stress $\tau_{yz}(x = 1.786, y = 23.214, z)$ for cross-ply lay-up 0/90/0

The calculations are performed for a three layer structure with a cross ply lay-up of [0/90/0]. One quarter of the plate is analyzed with regular meshes of 21×21, 63×63 elements of 4-node (model 1) and 9-node shell elements (model 2) taking into account symmetry conditions. Soft support for the rotational degrees of freedom are chosen as boundary conditions. The transverse shear stresses are evaluated at the center of elements at $(x, y, z) = (23.214, 1.786, z)\, mm$ for τ_{xz} and $(x, y, z) = (1.786, 23.214, z)\, mm$ for τ_{yz}.
For the 8-node solid shell element, we use a discretization of 14 x 14 elements and 8 elements in thickness direction of each layer. This relative fine discretization in thickness direction is necessary to get proper results. The results for model 1 and model 2 as well as the solid shell element are shown in Figs. 4 and 5. Note that the shear stresses are continuous at the layer boundaries. At the bottom surface and the top surface the stress boundary conditions are exactly fulfilled for model 1. There is good agreement between the different models.
The influence of a distorted mesh on the results has also been investigated. We compare results of a distorted mesh (1594 elements, 1675 nodes – produced with a meshing scheme based on an advancing front technique) with a regular mesh (1600 elements, 1681 nodes). Fig. 6 depicts the distribution in thickness direction for the transverse shear stresses τ_{xz} at $(x, y, z) = (24.7, 0.3, z)\, mm$ and Fig. 7 for τ_{yz} at $(x, y, z) = (0.3, 24.7, z)\, mm$. As expected the results are influenced by the distorsion, but not significantly.

The effect of the mesh distorsion on the distribution of the stress resultant q_x is plotted in Figs. 8 - 9, whereas Figs. 10 - 11 present the influence on the transverse shear stress τ_{xz} at $z = 0$. Only small differences occur.

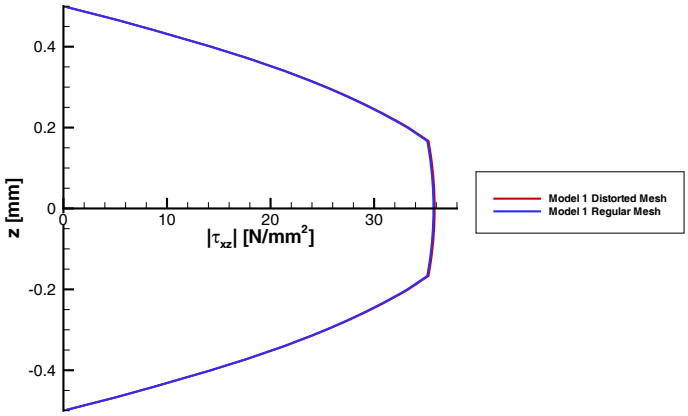

Figure 6: Shear stress $\tau_{xz}(x = 24.7, y = 0.3, z)$ for lay-up 0/90/0 in a regular and a distorted mesh

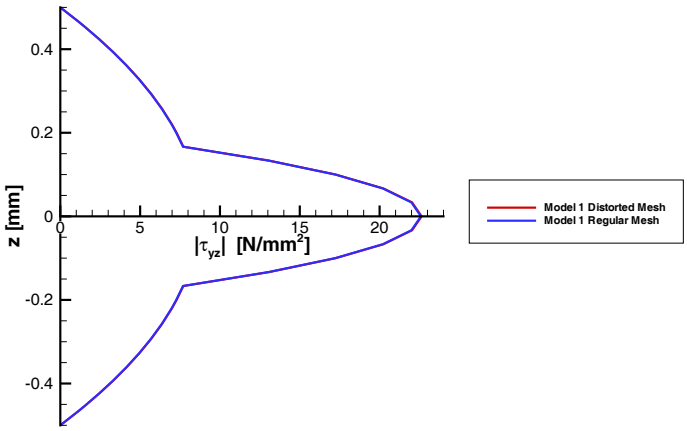

Figure 7: Shear stress $\tau_{yz}(x = 0.3, y = 24.7, z)$ for lay-up 0/90/0 in a regular and a distorted mesh

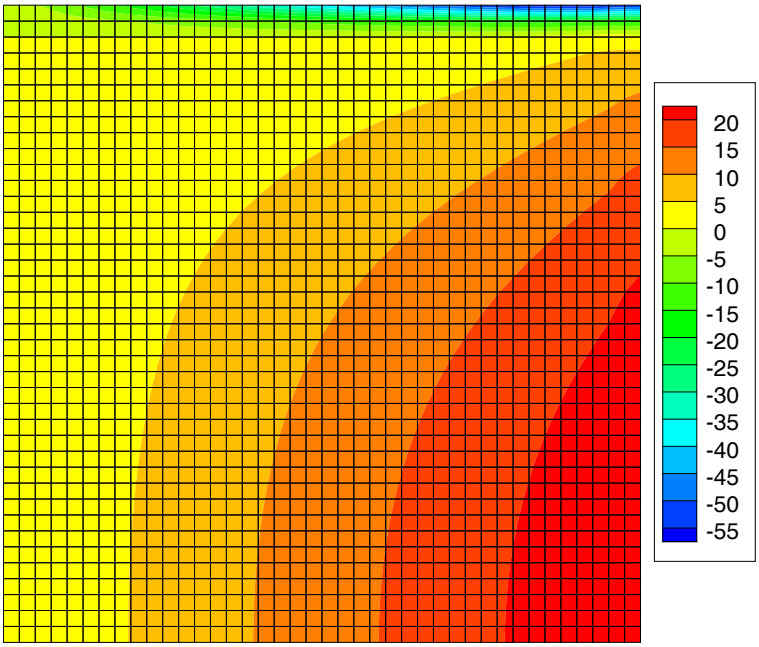

Figure 8: Stress resultant $q_x(x, y)$ in N/mm for lay-up 0/90/0 in a regular mesh

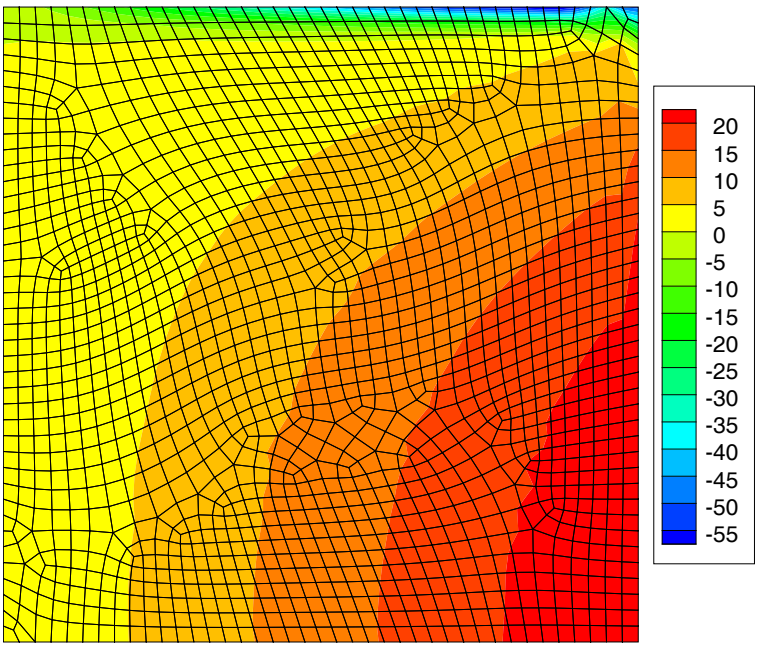

Figure 9: Stress resultant $q_x(x, y)$ in N/mm for lay-up 0/90/0 for a distorted mesh

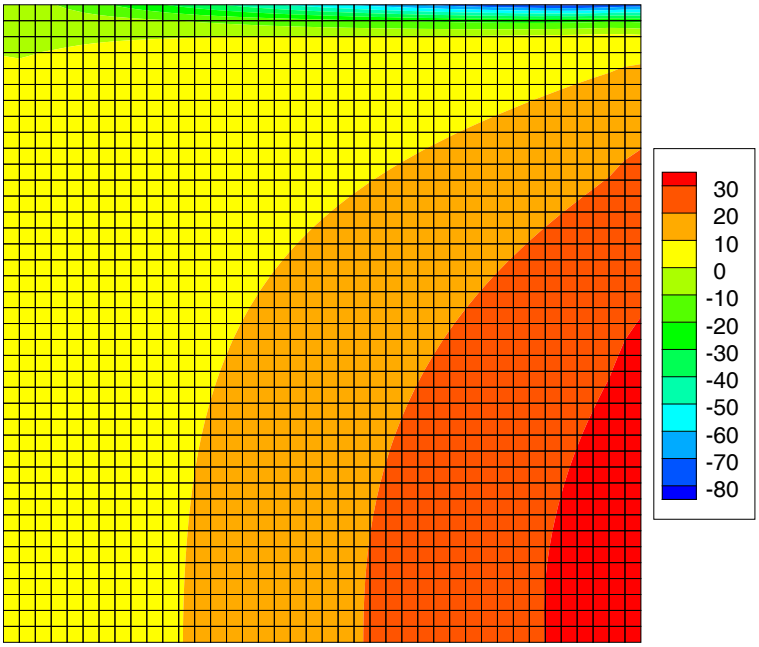

Figure 10: Shear stress $\tau_{xz}(x, y, z = 0)$ in N/mm^2 for lay-up $0/90/0$ in a regular mesh

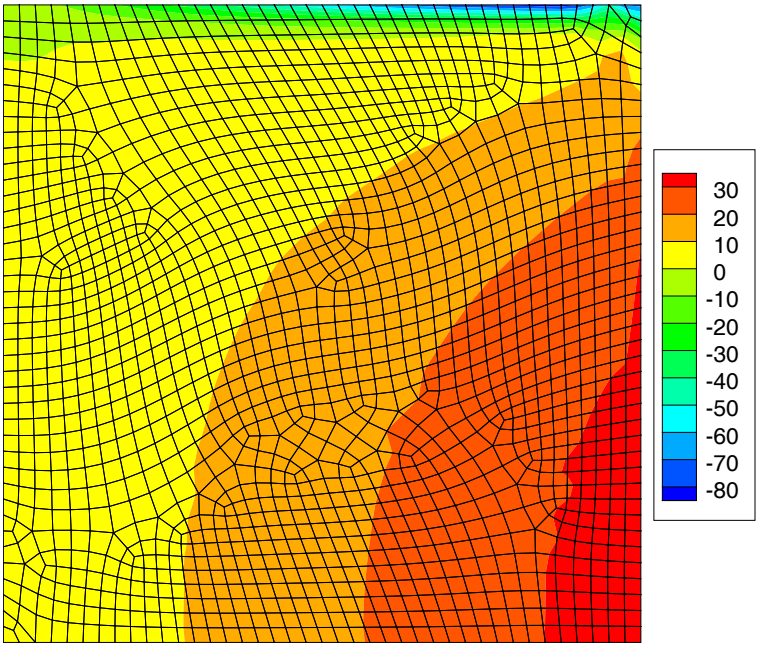

Figure 11: Shear stress $\tau_{xz}(x, y, z = 0)$ in N/mm^2 for lay-up $0/90/0)$ in a distorted mesh

5.2 Example 2

With the second example we present calculations for the same plate (geometry, boundary conditions and loading) with three layers but now with an angle play lay-up of [45/-45/45]. Thus, no longer symmetry conditions can be used.
The transverse shear stress τ_{xz} is evaluated at $(x, y, z) = (21.429, 0, z)\, mm$ and τ_{yz} at $(x, y, z) = (0, 21.429, z)\, mm$. The associated thickness distributions are shown in Figs. 12 and 13. For models 1 and 2 two meshes with 21×21 and 63×63 elements are used. For comparison we present results computed with solid shell elements [6]. Here a mesh with 42×42 elements and 7 elements for each layer is used. Again there is good agreement between the different models.

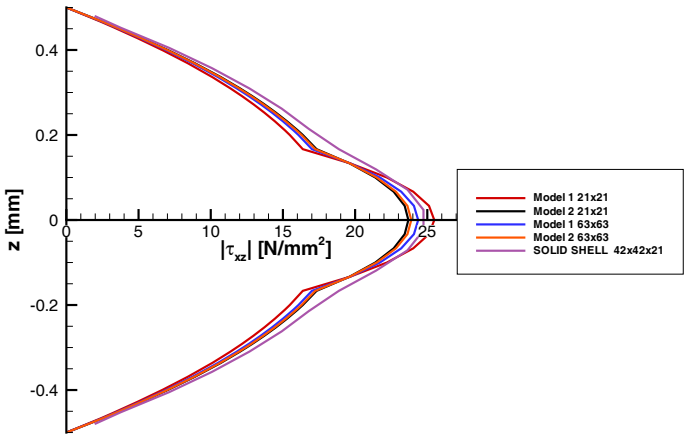

Figure 12: Shear stress $\tau_{xz}(x = 21.429, y = 0, z)$ for an angle ply lay-up 45/-45/45

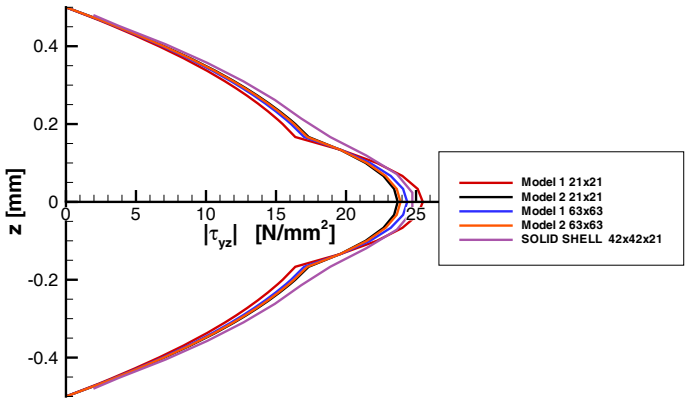

Figure 13: Shear stress $\tau_{yz}(x = 0, y = 21.429, z)$ for an angle ply lay-up 45/-45/45

A different shape of the transverse shear stresses is obtained at the coordinates $(x, y, z) = (10.937, 14.062, z)\, mm$. Figs. 14 and 15 show the results for τ_{xz} and τ_{yz} for model 1 and model 2 based on a discretization with 48×48 elements as well as for the solid shell element with a mesh of $32 \times 32 \times 24$ elements. In continuation to the previous results good agreement between the presented different strategies is observed.
The different curvature of τ_{xz} and τ_{yz} in the central layer follows from fact that the value of $\sigma_{x,x} + \tau_{xy,y}$ changes the sign in the central layer, whereas the value of $\sigma_{y,y} + \tau_{xy,x}$ possesses the same sign in all three layers.

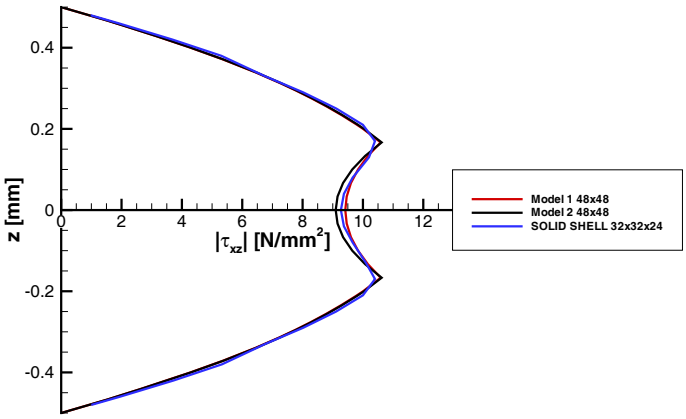

Figure 14: Shear stress $\tau_{xz}(x = 10.937, y = 14.062, z)$ for lay-up 45/-45/45

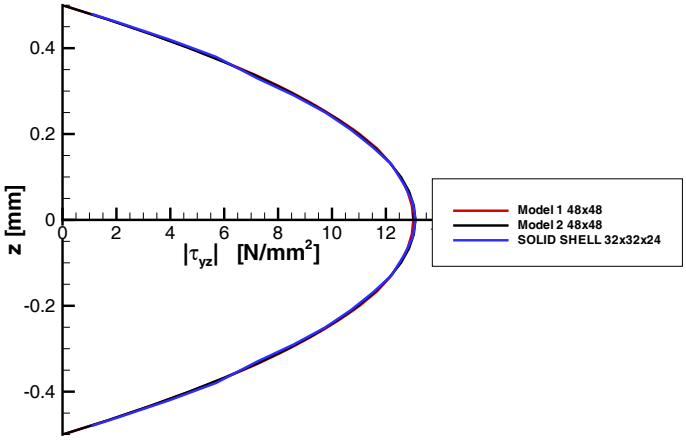

Figure 15: Shear stress $\tau_{yz}(x = 10.937, y = 14.062, z)$ for lay-up 45/-45/45

5.3 Example 3

The results for an unsymmetric lay-up are shown in Figs. 16 and 17. Again we consider the same plate (geometry, boundary and loading conditions), but now with two layers and a lay-up of [0/90]. Models 1 and 2 are applied with meshes using 21×21 and 63×63 elements. The mesh of solid shell elements consists of 28×28 elements in-plane and 8 elements for each layer. The transverse shear stresses τ_{xz} are evaluated at $(x, y, z) = (21.429, 0, z)\, mm$ and τ_{yz} at $(x, y, z) = 0, 21.429, z)\, mm$. The diagrams show that the results of the different models are in good agreement.

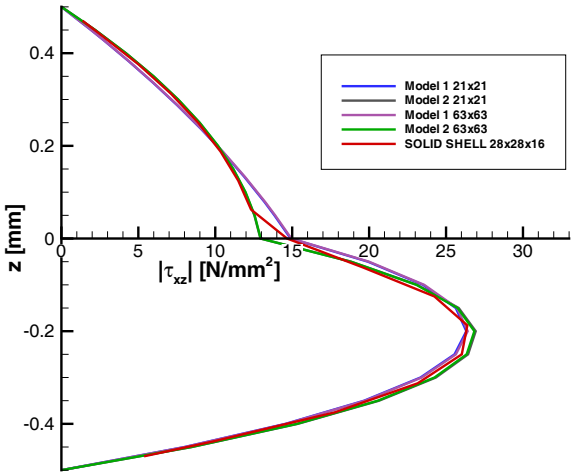

Figure 16: Shear stress $\tau_{xz}(x = 21.429, y = 0, z)$ for unsymmetric lay-up 0/90

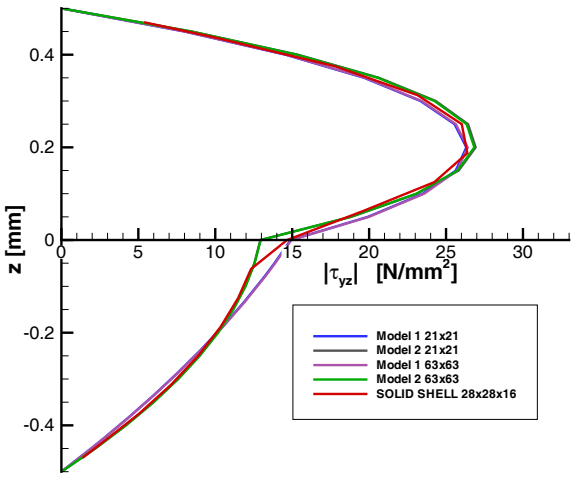

Figure 17: Shear stress $\tau_{yz}(x = 0, y = 21.429, z)$ for an unsymmetric lay-up 0/90

5.4 Example 4

With the last example with length-to-thickness ratio of $l_x/h = l_y/h = 10$ we consider a moderately thick plate. We choose $l_x = l_y = 10\,mm$ and thickness $h = 1\,mm$ and a layer sequence [0/90/0]. The plate is loaded by a sinusoidal load with a maximum value of $q = 1\,N/mm^2$ at the plate center. The boundaries are simply supported (hard support) along all edges, more precisely:

$$\begin{aligned} x = \pm l_x/2: \qquad & u_z = \theta_x = 0 \\ y = \pm l_y/2: \qquad & u_z = \theta_y = 0\,, \end{aligned}$$

where θ_x, θ_y denote the rotations about the $x-$ axis and $y-$ axis, respectively. Here, the origin of the coordinate system lies at the center of the plate. Again symmetry of the plate is considered when discretizing the structure. The mesh densities are chosen as in example 1. Shear stresses τ_{xz} are evaluated at $(x, y, z) = (4.643\,mm, 0.357\,mm, z)$ and τ_{yz} at $(x, y, z) = (0.357\,mm, 4.643\,mm, z)$. Figures 18 and 19 show that there is good agreement between the different models.

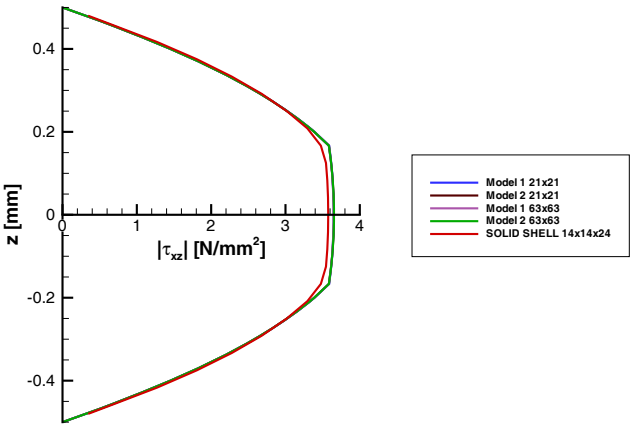

Figure 18: Shear stress $\tau_{xz}(x = 4.643, y = 0.357, z)$ for cross-ply lay-up 0/90/0

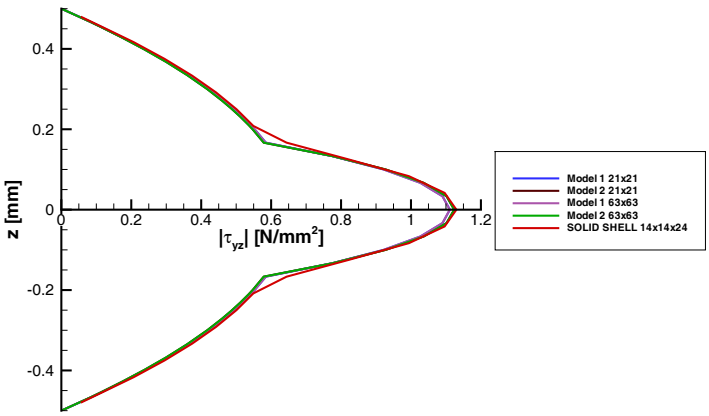

Figure 19: Shear stress $\tau_{yz}(x = 0.357, y = 4.643, z)$ for cross-ply lay-up 0/90/0

5.5 Sensitivity on the regularization parameter

Fig. 20 shows the dependency of some selected shear stresses on the normalized regularization parameter α^*. For the horizontal axis a logarithmic scale is chosen. The below defined shear stresses τ of examples 1 to 4 are computed at the specified coordinates x, y, z according to the following table:

Table 1: Definition of some selected shear stresses

Example	τ	x	y	z
1	$\lvert\tau_{yz}\rvert$	1.786	23.214	0
2	$\lvert\tau_{xz}\rvert$	21.429	0	0
3	$\lvert\tau_{xz}\rvert$	21.429	0	-0.2
4	$10 \cdot \lvert\tau_{yz}\rvert$	0.357	4.643	0

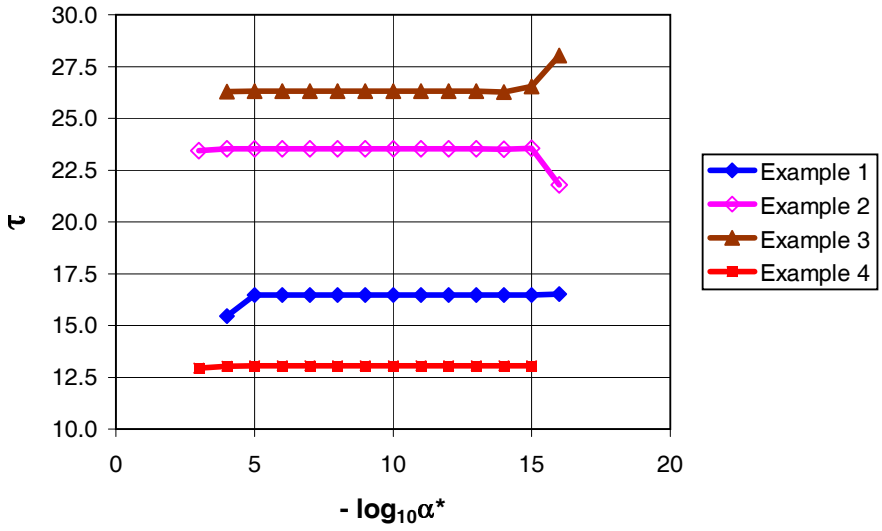

Figure 20: Sensitivity on the regularization parameter

In the range of $10^{-14} \leq \alpha^* \leq 10^{-5}$ the results are practically constant. Based on this investigation we choose an average value $\alpha^* = 10^{-10}$ for the computations.

6 Conclusions

The present paper deals with the calculation of transverse shear stresses in thin composite plate structures. For typically used 4-node elements a formulation has been introduced, which allows the evaluation of strain derivatives. The procedure is computationally effective since the required stiffness matrix has to be set up and factorized only once for a laminate with fixed lay-up. Several plate examples with symmetric and unsymmetric lay-ups are considered. The agreement with solutions obtained with 9-node elements and and with solutions obtained with 8-node solid shell elements is good. The computing time using the presented model is significantly less in comparison to three–dimensional finite element computations. The proposed models can not be applied to thick plates, since the underlying assumptions are not valid. Finally it is important to mention that also the interlaminar normal stresses are significant in the context of composite failure analysis. The effective computation of these stresses in layered plates has to be addressed in further research.

References

[1] Auricchio F, Sacco E (1999) A Mixed-Enhanced Finite-Element for the Analysis of Laminated Composite Plates. International Journal for Numerical Methods in Engineering 44:1481-1504

[2] Rohwer K (1992) Application of higher order theories to the bending analysis of layered composite plates. Int J Solids and Structures 29:105-119

[3] Degenhardt R, Rolfes R, Zimmermann R, Rohwer K (2006) COCOMAT - Improved MATerial Exploitation at Safe Design of COmposite Airframe Structures by Accurate Simulation of COllapse. Composite Structures 73:175-178

[4] Mittelstedt C, Becker W (2004) Interlaminar stress concentrations in layered structures, Part I: A selective literature survey on the free-edge effect since 1967. Journal of Composite Materials 38:1037-1062

[5] Marimuthu R, Sundaresan M K, Rao G V (2003) Estimation of Interlaminar Stresses in Laminated Plates Subjected to Transverse Loading using Three-dimensional Mixed Finite Element Formulation The Institution of Engineers(India), Technical Journal Aerospace Engineering 84:1-8

[6] Klinkel S, Gruttmann F, Wagner W (1999) A continuum based 3D-shell element for laminated structures. Computers & Structures 71:43-62

[7] Klinkel S, Gruttmann F, Wagner W (2006) A Robust Non-Linear Solid Shell Element Based on a Mixed Variational Formulation. Comp Meth Appl Mech Engng 195:179-201

[8] Reddy J N (1987) A Generalization of Two-Dimensional Theories of Laminated Plates. Communications in Applied Numerical Methods 3:173-180

[9] Chaudhuri R A (1986) An equilibrium method for prediction of transverse shear stresses in a thick laminated plate. Computers and Structures 23:139-146

[10] Carrera, E (1996) C^0 Reissner-Mindlin Multilayered Plate Elements Including Zig-Zag and Interlaminar Stress Continuity. International Journal for Numerical Methods in Engineering 39:1797-1820

[11] Brank B, Carrera E (2000) Multilayered shell finite element with interlaminar continuous shear stresses: a refinement of the Reissner-Mindlin formulation. Int J Num Meth Eng 48:843-874

[12] Carrera E (2003) Historical review of Zig-Zag theories for multilayered plates and shells. Applied Mechanics Reviews 56:237-308

[13] Gruttmann F, Wagner W, Meyer L, Wriggers P (1993) A Nonlinear Composite Shell Element With Continuous Interlaminar Stresses. Computational Mechanics 13:175-188

[14] Gruttmann F, Wagner W (1994) On the Numerical Analysis of Local Effects in Composite Structures. Composite Structures 29:1-12

[15] Gruttmann F, Wagner W (1996) Coupling of 2D- and 3D-Composite Shell Elements in Linear and Nonlinear Applications. Comp Meth Appl Mech Eng 129:271-287

[16] Gruttmann F, Wagner W (1996) Delamination Analysis of thin Composite Structures using a Multi-Director Formulation. in B.H.V. Topping(ed.) Adavances in Analysis and Design, Civil-Comp. Press, Edinburgh, 51-59

[17] Robbins D H, Reddy J N (1993) Modelling of thick composites using a layerwise laminate theory. Int J Num. Meth Eng 36:655-677

[18] Reddy J N (1984) A Simple High-Order Theory for Laminated Composite Plates. Journal of Applied Mechanics 51:745-752

[19] Engblom J J, Ochoa O O (1985) Through-the-thickness stress distribution for laminated plates of advanced composite materials. Int J Num Meth Eng 21:1759-1776

[20] Reddy J N (1989) On refined computational models of composite laminates. Int J Num Meth Eng 27:361-382

[21] Rao K M, Meyer-Piening H R (1990) Analysis of thick laminated anisotropic composite plates by the finite element method. Composite Structures 15:185-213

[22] Topdar P, Sheikh A H, Dhang N (2003) Finite Element Analysis of Composite and Sandwich Plates Using a Continuous Interlaminar Shear Stress Model J Sandwich Structures Materials, 5:207-231

[23] Noor A K, Burton W S, Peters J M (1990) Predictor-corrector procedure for stress and free vibration analyses of multilayered composite plates and shells. Comput Meth Appl Mech Eng. 82:341-364

[24] Noor A K, Kim Y H, Peters J M(1994) Transverse shear stresses and their sensitivity coefficients in multilayered composite panels. AlAA J 32:1259-1269

[25] Manjunatha B S, Kant T (1994) On evaluation of transverse stresses in layered symmetric composite and sandwich laminates under flexure. Engineering Computations 10:499-518

[26] Rolfes R, Rohwer K (1997) Improved transverse shear stresses in composite finite elements based on first order shear deformation theory. Int J Num Meth Eng 40:51-60

[27] Gruttmann F., Taylor R.L. (1992) Theory and Finite Element Formulation of Rubberlike Membrane Shells Using Principal Stretches, Int. J. Num. Meth. Engng. 35:1111-1126

[28] Gruttmann F, Wagner W (2006) Structural analysis of composite laminates using a mixed hybrid shell element. Computational Mechanics 37:479-497

[29] Taylor RL Feap - manual. http:\\www.ce.berkeley\ ∼rlt\feap\manual.pdf

[30] Schenk O, Gärtner K (2004) Solving Unsymmetric Sparse Systems of Linear Equations with PARDISO. Journal of Future Generation Computer Systems 20,3: 475-487